

Article

Thermal Environment Control at Deep Intelligent Coal Mines in China Based on Human Factors

Qiaoyun Han ^{1,*}, Debo Lin ¹, Xiaojie Yang ^{2,3}, Kongqing Li ¹ and Wei Yin ¹ ¹ School of Civil Engineering, Hunan University of Science and Technology, Xiangtan 411201, China² State Key Laboratory for Geomechanics and Deep Underground Engineering, China University of Mining and Technology-Beijing, Beijing 100083, China³ School of Mechanics and Civil Engineering, China University of Mining and Technology-Beijing, Beijing 100083, China

* Correspondence: lyxc43@163.com

Abstract: Mechanical cooling of the entire mining tunnel, widely used in deep coal mines, has a significant energy-intensive consumption, particularly for intelligent mining tunnels. Therefore, localized cooling would benefit the intelligent mining industry. Current studies on the temperature, relative humidity, and air velocity under localized cooling for working protection are still unclear. A modified predicted heat strain model that is appropriate for warm and humid conditions is presented in this article and calculated using MATLAB. Results reveal that air temperature was the primary factor affecting underground miners' safety. Increasing air velocity would improve the working environment when the thermal humidity index is lower than 32. Reducing total working time and wet bulb temperature would benefit underground miners' security. For the cooling of intelligent mining tunnels, the recommended air velocity would be 2 m/s, and the maximum wet bulb temperature would be 28 °C for the 6-h working period and 26 °C for the 8-h working period. Results would be beneficial to the cooling of intelligent mining in China.

Keywords: intelligent mining; exposure duration; PHS model; warm and humid environment; localized cooling



check for updates

Citation: Han, Q.; Lin, D.; Yang, X.; Li, K.; Yin, W. Thermal Environment Control at Deep Intelligent Coal Mines in China Based on Human Factors. *Sustainability* **2023**, *15*, 3193. <https://doi.org/10.3390/su15043193>

Academic Editors: Ying Sheng and Chunxiao Su

Received: 22 November 2022

Revised: 13 January 2023

Accepted: 6 February 2023

Published: 9 February 2023



Copyright: © 2023 by the authors. Licensee MDPI, Basel, Switzerland. This article is an open access article distributed under the terms and conditions of the Creative Commons Attribution (CC BY) license (<https://creativecommons.org/licenses/by/4.0/>).

1. Introduction

The Chinese mining industry is dominated by deep underground mining [1,2]. Intelligent mining technology based on automatic mining methods was developed to respond to excessive energy consumption, low productivity, and high safety risks associated with traditional mining in China. Over 900 fully automated coal extraction faces are currently in operation [3]. Intelligent mining entails fewer underground workers and a lower metabolic rate, as shown in Tables 1 and 2.

Mechanical cooling systems have been most frequently used in the thermal environment due to deep mining [2,4]. However, cooling an entire tunnel would be a significant energy-intensive process, accounting for up to 25% of total electricity consumption [4]. Moreover, the reduction in the number of workers and decreased physical work intensity suggest that localized cooling is widespread in the intelligent mining industry. Consequently, the climatic conditions under localized cooling will be studied.

Nations worldwide have focused on controlling the thermal environment under deep mines, as shown in Table 3. Vosloo et al. [5] reported that underground working areas require WBT below 27.5 °C. Twort et al. [6] determined that ET 28.8 °C was the upper climatic design limit. Belle et al. [7] recommended lowering WBT below 27 °C to reduce the risk of heat stroke. Han et al. [8] showed that when the relative humidity is reduced to 60%, even the DBT of 30 °C satisfies the workers in the entire tunnel. Rohanchi et al. [9] found that a velocity of 1–2 m/s is ideal for guaranteeing the workers' thermal comfort. Haiqiao et al. [10] stated that reducing RH would improve thermal comfort in deep mines. Shugang et al. [11]

reported that the DBT in deep mines could be extended up to 28 °C. Saunders et al. [12] presented that 33 °C and 60% RH would be acceptable. Paloma Lazaro et al. [13] proposed a modified PHS model for deep mines. Sasmito et al. [14] found that DBT significantly impacts temperature distribution throughout the tunnel. Xingxin et al. [15] suggest that miners are most comfortable when temperatures are below 27 °C, humidity is between 60% and 70%, and wind speeds are at least 0.5 m/s. Telebi et al. [16] found that increasing clothing insulation lowers the maximum exposure time. Kalkowsky et al. [17] measured miners' heart rates and rectal temperatures. Jinggang et al. [18] determined that the critical tolerable temperature and relative humidity were 37 °C and 80%, respectively. Chao et al. [19] demonstrated that it is necessary to stop working under heavy and cumbersome loads under WBGT over 35 °C. Jiasong et al. [20] found that increasing air velocity (less than 2 m/s) would increase miners' exposure. Chenqiu et al. [21] proposed modifying inputs to improve the prediction of the PHS model underground. Sunkpal et al. [22] determined that the optimal air velocity for thermal comfort was 1.5 m/s. Zhaoxiang et al. [23] presented a classification criterion for assessing underground airway heat hazards. Zijun et al. [24] found that the temperature of the surrounding rock is the most significant factor in the release of latent heat and sensible heat. Jiuzhu et al. [25] report that ventilation temperature influences DBT the most. Dingyi et al. [26] studied heat stress with nine evaluation indexes. Ji et al. [27] concluded that the maximum safe working time is 4 h at 32 °C and 90% RH. According to Qianming et al. [28], workers in deep mines should be protected from high temperatures by a DBT of 27 °C.

Table 1. Mining workers in a work shift.

Intelligent Mining Faces	Workers (People/8 h)	
	Traditional Mining	Intelligent Mining
1306 mining face, Licun Coal mine	28	16
1001 mining face, Huangling 1# Coal mine	11	3
1008 mining face, Fumei Coal mine	12	5
5# Xiangshan Coal mine	25	10
214,201 mining face, Hanjiawan Coal mine	15	6
7302 mining face, Yanzhou Coal mine	25	7
74,104 mining face, Zhangshuanglou Coal mine	16	5

Table 2. Metabolic rate of the mining workers.

Occupations	Metabolic Rate (W/m ²)	Traditional Mining	Intelligent Mining
Inspector	160	✓	✓
Driver	160	✓	✓
Maintenance engineer	160	✓	✓
Coal cleanup workers	300	✓	×
Workers at the head and tail of coal-cutter	250	✓	×
Workers for the hydraulic supports	250	✓	×

The experts have agreed that the thermal environment under the deep mine needs to be improved. Unfortunately, the thermal environment-controlling conditions proposed did not agree with each other due to inconsistent heat stress indicators. Considering the safety and health of mining workers, a modified PHS model for a warm and humid climate would be more suitable for evaluating underground mines during intelligent mining. This paper presents and calculates a modified PHS model for a warm and humid climate using the MATLAB program. The impact of environmental parameters on maximum exposure

duration was then examined. Lastly, raise the parameters for localized cooling at Jiahe Coal Mine.

Table 3. Thermal environment controlling measures.

Country	Environmental Conditions
China	When the DBT exceeds 30 °C, production must be stopped.
United States	Upper WBT of 30 °C for unimpaired performance on sedentary tasks and 28 °C for moderate levels of physical work.
Australia	WBT ≤ 28 °C
France	Synthesizing temperature < 28 °C
Germany	1. When DBT > 28 °C or ET > 25 °C <ul style="list-style-type: none"> • ET of 25–29 °C lasts for 3 h a day, working time should not exceed 6 h; • ET of 29–30 °C lasts for 2.5 h a day, working time should not exceed 5 h; • People would not be allowed to work when ET exceeds 30 °C. 2. Staff members aged under 21 or over 50 would be prohibited from working at the environment with ET exceeding 29 °C.
Great Britain	When the ET exceeds 28 °C, the working time would be no longer than 1.5 h. Semi-mechanization working face: ET ≤ 27.2 °C; Mechanized working face: ET ≤ 28.3 °C ET ≤ 30.0 °C: light levels of physical work; ET ≤ 28.0 °C: moderate levels of physical work; ET ≤ 26.5 °C: heavy levels of physical work.
Poland	When DBT > 26 °C, the workload should be reduced by 4%; DBT > 28 °C, working time should be no longer than 6 h; DBT > 33 °C, only ambulance work is allowed.
India, Italy	DBT ≤ 32 °C
Japan	DBT ≤ 30 °C in the mining face and 31 °C for heading face.
South Africa	WBT ≤ 27.5 °C
Former Soviet Union	When RH ≥ 90%, the allowable DBT was 25 °C if air velocity was larger than 2 m/s and no more than 24 °C if the air velocity was smaller than 1 m/s.

2. Materials and Methods

DBT, RH, clothing insulation, exposure duration, and metabolic rates determine the heat effect on a mining worker. Heat illness occurs when heat stress exceeds the resultant heat strain. As a result, it is becoming increasingly significant to assess underground environmental conditions according to the allowable heat stress for the security of miners.

Heat gains and losses by the human body are expressed in the heat balance equation [29]. Figure 1 and Equation (1) illustrate that heat storage (S), which accumulates in the body, is the metabolic rate's (M) less adequate mechanical power (W), as well as heat exchanges due to conduction (K), convection (C), radiation (R) and evaporation (E).

$$S = M - W - K - C - R - E \quad (1)$$

People would be comfortable when S equals zero. When $S > 0$, heat accumulates in the body, leading to a rising rectal temperature and water loss. Rectal temperature and water loss have been calculated using the PHS model in ISO 7933. ISO 7933 suggests that the maximum rectal temperature for workers is 38 °C and the maximum water loss is 7.5% of body mass. Mining companies and experts agree that the PHS index is a handy tool for evaluating and managing occupational heat exposures [13]. Most coal miners suffer from high temperatures and high humidity working under mine tunnels, where DBT is over 30 °C and RH is close to 100% [2,10]. Enzymatic activity increases when the body is exposed to a 30–45 °C environment, and chemical reactions accelerate [30]. During sweating, some sweat is absorbed into the clothes, causing a change of the clothes' insulation, and the evaporated one causes a change in evaporation heat resistance. ISO 7933 simplifies metabolic rate, clothing insulation, and evaporation heat resistance as constants, resulting in inaccurate predictions of human heat tolerance under deep hot and humid conditions. The schematic diagram can be found in Figure 2.

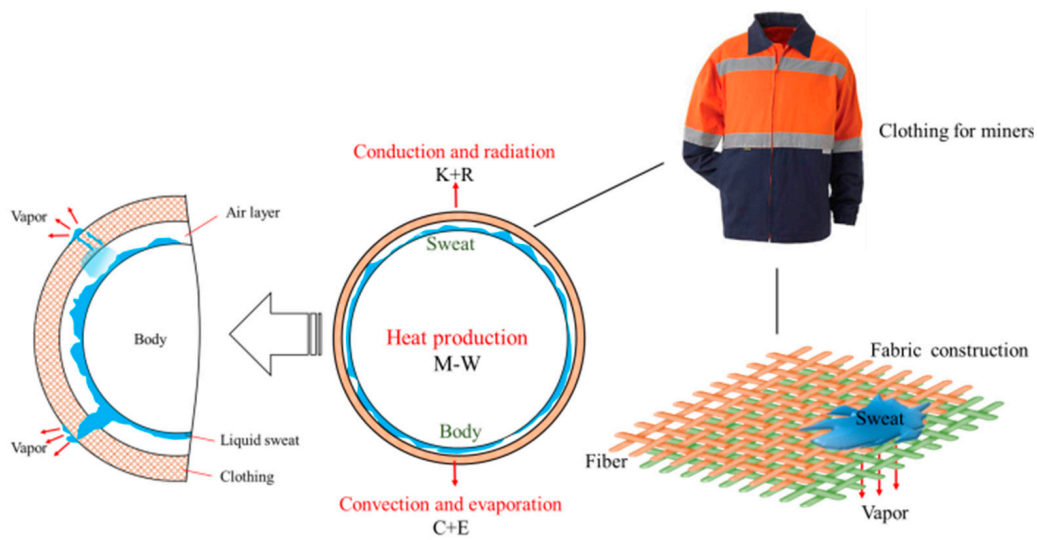


Figure 1. Heat balance of the human body.

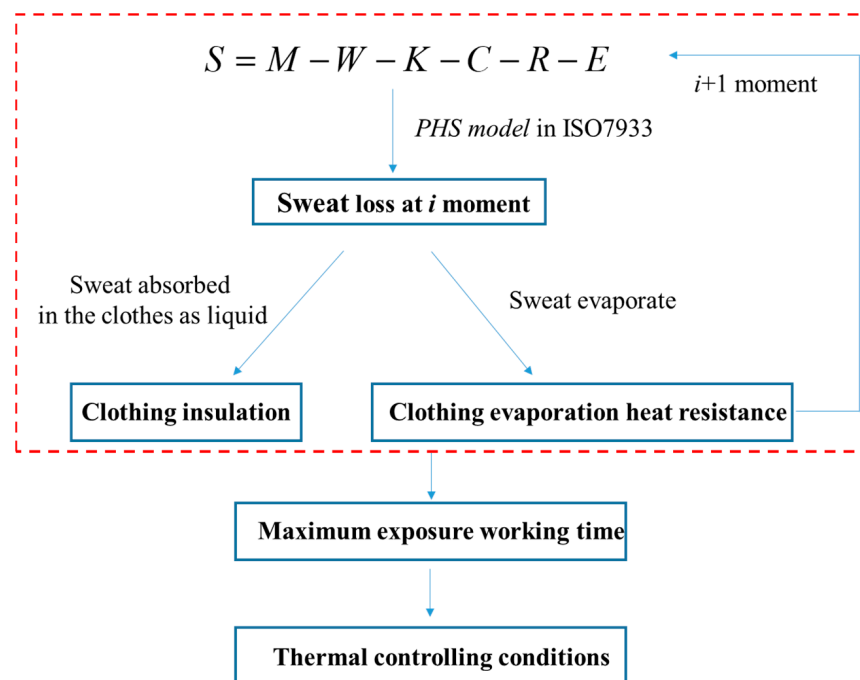


Figure 2. Schematic diagram of the article.

2.1. Metabolic Rate of the Miners under Hot and Humid Mine

Metabolism measures the energetic cost of muscular load and is used as an activity indicator because it converts chemical energy to mechanical and thermal energy. Enzymatic activity increases when the body is exposed to 30–45 °C, and chemical reactions accelerate [30,31]. As a result, the empirical values provided by ISO 8996 cannot be applied to hot and humid conditions. Xiaoli et al. [32] found that a maximum increase of 5 to 10 W/m² would be expected in the hot climate due to increased heart rate and sweating. Werner et al. [33] demonstrated that M is a function of time and local coordinates in three dimensions. Experiments collected from previous studies [34–36] in a warm and humid environment (heart rate, respiratory quotient, oxygen consumption rate, carbon dioxide production, etc.) were used to calculate the actual metabolic rate (Ma) in a hot and humid

environment utilizing Equations (2)–(5). Comparing the Ma and ISO8996 (Mexp), we found that the ΔM should be 20–30%.

$$M = \frac{HR - HR_0}{RM} + M_0 \quad (2)$$

$$RQ = \frac{\dot{V}_{CO_2}}{\dot{V}_{O_2}} \quad (3)$$

$$EE = 5.88 \cdot (0.23 \cdot RQ + 0.77) \quad (4)$$

$$M = EE \times \dot{V}_{O_2} \times \frac{1}{A_{Du}} \quad (5)$$

$$\Delta M = \frac{M_a - M_{exp}}{M_{exp}} \quad (6)$$

M_0 —metabolic rate at rest, W/m²;
 HR—heart rate, in beats per minute;
 HR₀—heart rate, in beats per minute;
 RM—increase in heart rate per unit of metabolic rate;
 RQ—respiratory quotient;
 \dot{V}_{O_2} —oxygen consumption rate, L/h;
 \dot{V}_{CO_2} —carbon dioxide production, L/h;
 A_{Du} —body surface area, m².

2.2. Modified Clothing Insulation (Icl) and Evaporation HEAT resistance (R_t)

Thermal balance is achieved by transferring sweat from the skin surface to the air in liquid and gaseous forms. Sweat is absorbed in clothes as a liquid; then, the insulation changes, and some evaporates, altering the evaporation heat resistance. Accordingly, we proposed:

- (1) No sweat remains on the skin's surface;
- (2) Fabric volume was constant;
- (3) Heat conduction occurs when heat is transferred from the inside to the outside fabric;
- (4) The clothing fabric is made of 100% cotton.

Cotton fiber diameter increases when cotton fibers absorb water. Moisture regain is calculated when it exceeds the maximum water capacity (C_m).

$$\varepsilon = 1 - \frac{\rho_t}{\rho_s} \quad (7)$$

$$C_m = \frac{\rho_w}{\rho_s} \frac{\varepsilon_d}{1 - \varepsilon_d} \quad (8)$$

where ρ_t , ρ_w and ρ_s , respectively, indicated the density of fabric, water and fiber, g/cm³. ε_d represents the porosity factor when the clothing was completely dry.

As the fabric is porous, heat transfer in the clothing (Q) is divided into conduction through the air in the pores (Q_a), sweat in the pores (Q_w), and fibers (Q_s).

$$Q = Q_a + Q_w + Q_s \quad (9)$$

Fourier's law states:

$$Q_j = \frac{\lambda_j A_j \Delta t}{\delta} \quad (10)$$

where subscript *j* represents air, fiber and sweat; λ , λ_s , λ_a and λ_w , respectively, indicate the thermal conductivity of clothing, fiber, air and water, J/m·°C. Δt was the temperature

difference between the inside and outside of the clothing, °C. δ was the thickness of the clothing.

If water mass (m_w) ratio to fiber mass (m_s) in clothing is less than C_m , that is, $\frac{m_w}{m_s} < C_m$, water volume fraction in the fabric was supposed as x ; otherwise, the moisture content of the clothing (μ) would be a constant value C_m .

Total weight of the clothing at the i moment (m_i) was expressed as in Equation (11).

$$m_{wi} + m_s = m_i \quad (11)$$

$$m_{i+1} = (swt_{i+1} - m_{zi} - m_{si}) \cdot \Delta t + m_i \quad (12)$$

$$swt_i = m_{zi} + m_{si} + m_{li} \quad (13)$$

where,

m_i —Total weight of the clothing at the i moment, kg;

swt_i —Total sweat at the i moment, kg/s;

m_{zi} —Sweat that enters the air as a gas through a fabric, kg/s;

m_{si} —Sweat evaporating from the outer surface of the garment, kg/s;

m_{li} —Sweat remaining in the fabric;

Δt —Iteration interval, 60 s.

$$m_{wi} = \mu m_i \quad (14)$$

The simultaneous Equations (9)–(14) were derived and the following results were obtained:

$$\lambda = (1 - \varepsilon)\lambda_s + (\varepsilon - x)\lambda_a + x\lambda_w \quad (15)$$

$$x = \frac{\mu(1 - \varepsilon)\rho_s}{\rho_w(1 - \mu)} \quad (16)$$

Equation (17) specifies the clothing insulation (I_{cl}), whereas I_{cl0} refers to the initial clothing insulation, Clo.

$$I_{cl} = 0.155 \cdot \frac{\delta}{\lambda} \quad (17)$$

$$I_{cl0} = 0.161 + 0.835 \sum I_{clu0} \quad (18)$$

ISO 9920 suggests mining clothing parameters in Table 4. I_{clu0} of mining cloth was given in Table 5, and the I_{cl0} calculated as in Equation (18) was 0.57 clo. Figure 3 shows the results of several studies that have verified the model's reliability [37,38].

Table 4. Mining clothing parameters.

Material	Fabric Insulation (m ² ·KW ⁻¹)	Fabric Surface Density (g/m ²)	Thickness/mm
Denim/twill weave	0.023	206	0.8

Table 5. Insulation for typical clothing ensembles (ISO 9920).

Clothing Ensemble	I _{clu} /clo
Briefs	0.04
Long sleeves	0.16
Work pants	0.24
Socks	0.02
shoes	0.02
Cap	0.01

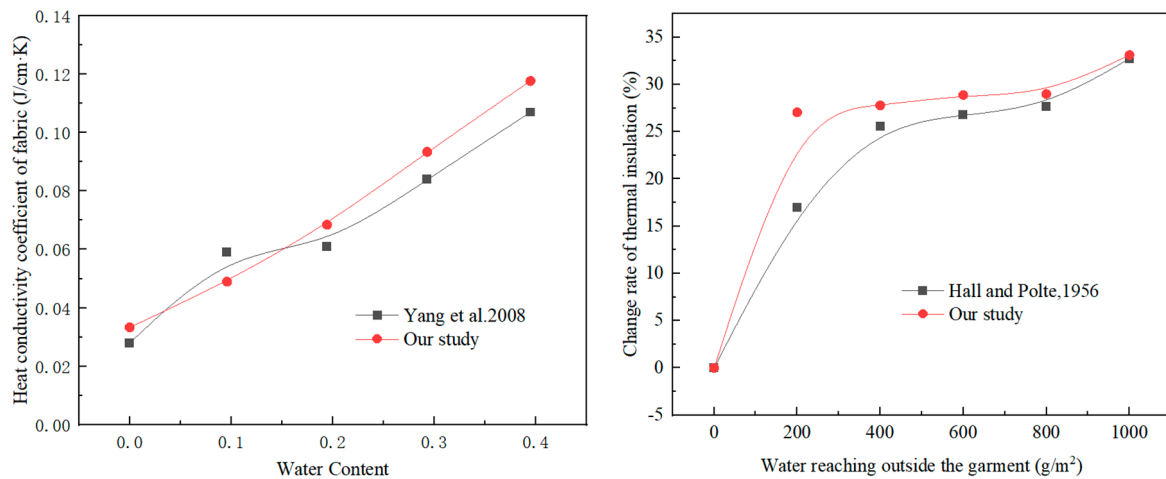


Figure 3. Verification of our model with the present studies.

$$I_{cl} = I_{cl0} \cdot \left(0.41 + 0.29e^{-\frac{m_{ji}}{885.73}} + 0.31 \cdot e^{-\frac{m_{ji}}{162.88}} \right) \quad (19)$$

According to the assumption, sweat equals the mass of water remaining in the clothing plus water evaporated from the skin and outer surface of the dress. As a consequence of the mass transfer process and the ideal gas state equation, m_{zi} would be expressed as follows.

$$m_{zi} = \frac{h_m}{R_w \cdot T_{cl}} (P_a - P_{cl}) \cdot A_i = \frac{(P_{cl} - P_{sk})}{R_{zi}} \quad (20)$$

$$\begin{aligned} R_{zi} &= \frac{R_w \cdot T_{sk}}{h_m \cdot A_i} \cdot \frac{(P_{cl} - P_{sk})}{(P_a - P_{cl})} \\ &= \frac{R_w \cdot T_{sk}}{h_m} \cdot \frac{\delta}{\varepsilon_i \cdot V} \cdot \frac{(P_{cl} - P_{sk})}{(P_a - P_{cl})} \end{aligned} \quad (21)$$

$$R_{ti} = \frac{R_{zi}}{r} \quad (22)$$

and because of

$$\varepsilon_i = \varepsilon_0 - x_i \quad (23)$$

Then,

$$m_{si} = \frac{h_m}{R_w \cdot T_{cl}} (P_a - P_{cl}) \cdot \left(\frac{V}{\delta} - A_i \right) \quad (24)$$

Imagine the human body as a cylindrical shape; the Re , Sc were calculated using Equations (25) and (26).

$$h_m = \frac{Sh \cdot D_a}{d} \quad (25)$$

$$Sh = 0.26Re^{0.6} Sc^{0.38} \left(\frac{Sc_{\infty}}{Sc_{cl}} \right)^{0.25} \quad (26)$$

where

h_m —Mass transfer coefficient, m/s;

T_{cl} —Water vapor saturation temperature of a garment's outer surface, K;

R_w —Constant of water vapor gas, 461.89 J/(kg·K);

P_{cl} —Water vapor pressure on the outer surface of the garment, Pa;

P_a —Water vapor pressure in roadway air, Pa;

P_{sk} —Water vapor pressure on the surface of the skin, Pa;

A_i —effective evaporation area, m²;

R_{zi} —Moisture vapor resistance at i moment, Pa·s/kg;

R_{ti} —Evaporative resistance of clothing at i moment, kPa·m²/W;

r —latent heat of vaporization, J/kg;

d —the diameter of the bottom surface, 0.3 m;
 D_0 —Coefficient of diffusion, cm^2/s ; u —air velocity, m/s.

2.3. Model Verification

Previous experiments have validated the modified PHS model [39–41]. The experiment results and predictions are listed in Tables 6–8. The error rate between the experiment results and predictions was significantly lower than 10%, implying an acceptable amount of error in the theoretical calculation.

Table 6. Model validation with study of Shapiro et al. [39].

Clothing	Walking Speed (m/s)	Treadmill Grade (%)	Sweat Loss ($\text{g}/(\text{m}^2 \cdot \text{h})$)	Predicted Sweat Loss ($\text{g}/(\text{m}^2 \cdot \text{h})$)	Error Rate (%)
Fatigue	Rest	-	198 ± 15	193.94	2.05%
Fatigue	1.34	0	580 ± 31	540.44	6.82%
Fatigue	1.34	5	691 ± 41	644.76	6.69%
Shorts	Rest	-	164 ± 16	156.69	4.46%
Shorts	1.34	0	386 ± 43	415.89	7.74%
Shorts	1.34	5	556 ± 23	594.58	6.94%

Table 7. Model validation with study of Qingqing et al. [40].

Clothing	Walking Speed (m/s)	Sweat Loss ($\text{g}/(\text{m}^2 \cdot \text{h})$)	Predicted Sweat Loss ($\text{g}/(\text{m}^2 \cdot \text{h})$)	Error Rate (%)	
Still conditions	0.56	0	28	30.45	8.76%
	0.6	0	35	38.45	9.86%
	0.68	0	50	50.65	1.29%
Activity 1	0.56	0.8	38	41.69	9.72%
	0.6	0.8	43	43.04	0.10%
	0.68	0.8	52	54.62	5.04%
Activity 2	0.56	1.2	53	57.69	8.86%
	0.6	1.2	59	58.96	0.06%
	0.68	1.2	70	69.60	0.58%

Table 8. Model validation with study of Mehnert et al. [41].

Parameters	Experiment 1	Experiment 2
Number of subjects	58	56
Ta ($^{\circ}\text{C}$)	32	25
RH (%)	50–55	50–55
Icl	0.6	0.85
Total sweat loss (g/m^2)	261	232
Predicted sweat loss (g/m^2)	264	221
Error rate (%)	1.2%	4.7%

An experiment by Shapiro et al. [39] involved 34 male soldiers dressed in T-shirts, shorts, socks, and indoor shoes. The average age of volunteers was 22.1 years old, weighing 71.3 kg and 176.4 cm tall. Each exposure lasted 120 min: 10 min of walking, followed by 10 min of rest, followed by a 50-minute walk or 120 min of continuous rest for the resting group. The ambient temperature was 35°C , and the relative humidity was 75%.

Twenty college students (mean values: age: 23.5 years; height: 167.7 cm; weight: 57.6 kg) were recruited for the experiments of Qingqing et al. [40]. The maximum metabolic rates of activities 1 and 2 were, respectively, 1.8 and 2.6 met. DBT was 30°C and RH was 52% during the investigation.

According to Mehnert et al. [41], subjects sat in a wire chair in a reclining position in experiment 1 and a standard car seat with a four-point seat belt in experiment 2.

3. Results and Discussion

The modified PHS model was calculated using MATLAB, and the parameters are listed in Table 9. Resting times would affect the maximum exposure duration and cooling parameters. However, the resting time at the coal mines we considered for cooling, for example, the Zhangshuanglou Coal Mine [8], Jiahe Coal Mine, and Zhangxiaolou Coal Mine [42], was irregular. People would take a break between jobs or when they felt fatigue. Moreover, we investigated additional coal mines in China for resting time and found the same results, as shown in Table 10. As a result, resting time should have been included in our article.

Table 9. Calculating parameters.

Calculating Parameters	Values
Weight/kg	65
Height/m	1.72
$M_{exp}/W/m^2$	160
I_{cl0}/clo	0.57
DBT/°C	16–50
RH/%	60–95
Air speed $u/m/s$	1–4
Walking Speed $W_a/m/s$	1
Duration/minutes	480

Table 10. Resting time of underground mining workers at coal mines in China.

Coal Mine	Work Shift	Resting Time/Minutes
Hongyang 3# Coal Mine	Three eight-hour shifts	30
Dongqu Coal Mine	Four six-hour shifts	0
Jinggong Coal Mine	Three eight-hour shifts	20–30
Longwanggou Coal Mine	Three eight-hour shifts	30
Liuyuanzi Coal Mine	Three eight-hour shifts	≤25
Hecaogou Coal Mine	Three eight-hour shifts	30
Zhangshuanglou Coal Mine	Three eight-hour shifts	almost 30
Jiahe Coal Mine	Three eight-hour shifts	almost 30
Zhangxiaolou Coal Mine	Three eight-hour shifts	almost 30
Sanhejian Coal Mine	Three eight-hour shifts	almost 30
Zhangji Coal Mine	Three eight-hour shifts	almost 30
Zhouyuanshan Coal Mine	Three eight-hour shifts	almost 30

3.1. Exposure Duration of Miners in the Hot and Humid Mine

Thermal humidity index (THI) [43] is used for the evaluation of the thermal environment.

$$THI = T_a - 0.55 \cdot (1 - RH) \cdot (T_a - 14.5) \quad (27)$$

When the THI is more than 32 (Figure 4(5),(6)), S will increase, and the critical physiological index will shortly be reached; therefore, workers will not be able to have heat blown away by increasing wind speeds. When the THI is lower than 32, increasing air velocity will improve the working environment, but the action becomes insignificant when the wind speed increases above 2 m/s. Moreover, our previous study [44] estimated that an air speed of 2 m/s would be the most negligible wind speed capable of dispersing the haze. Consequently, a 2 m/s air velocity should be recommended while localized cooling occurs in the tunnel.

DBT and RH have a negative impact on exposure duration, as seen in Figure 4. A variance analysis was conducted using SPSS22.0 software to assess the effect of environmental factors on exposure duration. Exposure duration was analyzed as a dependent variable, while environmental conditions were analyzed as an independent variable. Results in Table 11 indicate that exposure duration is most affected by DBT.

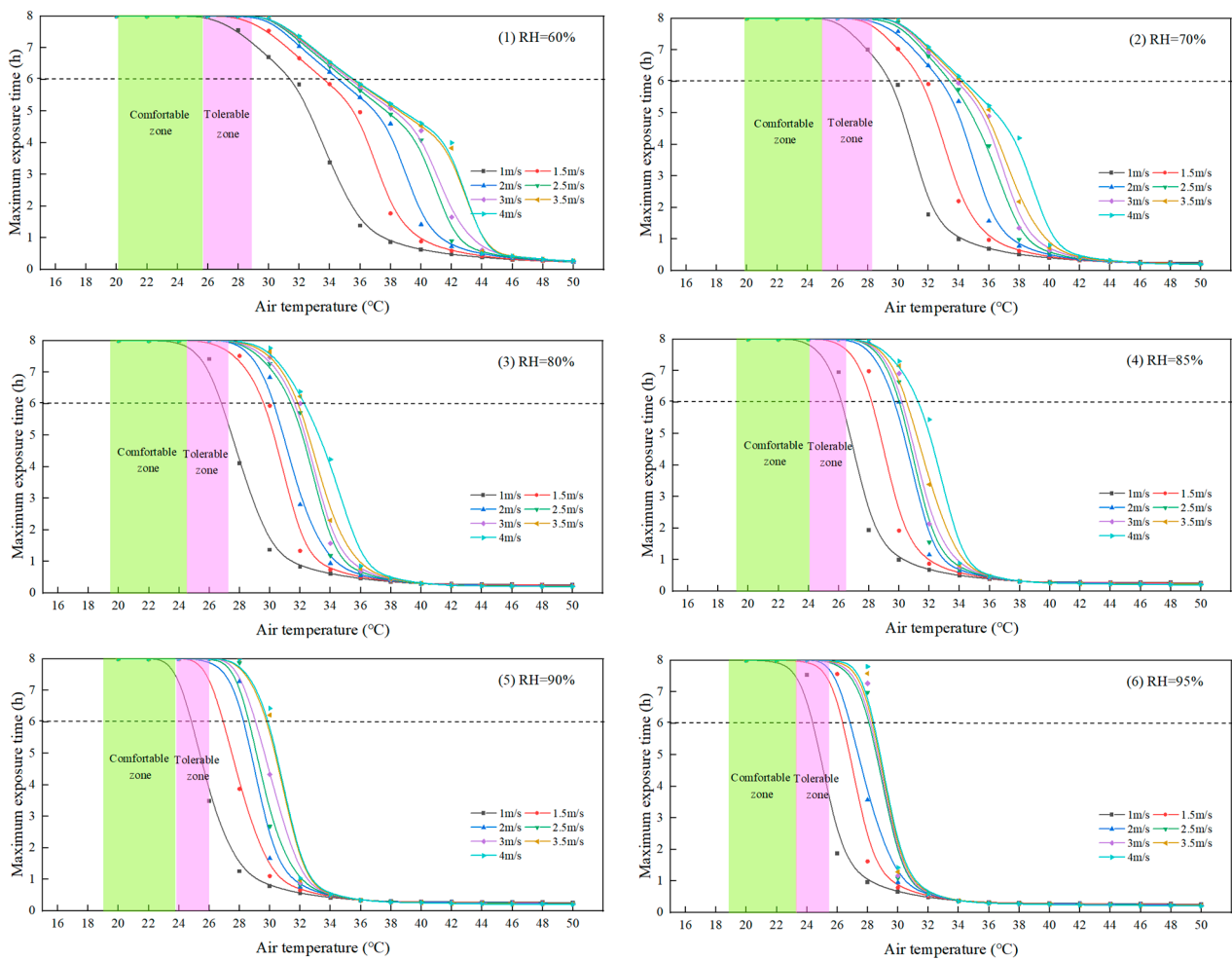


Figure 4. Exposure time of miners under different environmental conditions.

Table 11. Variance analysis of the effects of environmental factors.

Source	Type III Sum of Squares	Degrees of Freedom	Mean Square	F	Salience
Corrected model	5197	20	259.8	230	0.000
Intercept	29,256	1	29,256	25,921	0.000
DBT	4816	6	802.7	713.5	0.000
RH	625	4	156.3	139.5	0.000
Wind speed	798	5	159.6	145.4	0.000
Error	995	911	1.1		
Total	41,687	895			
Corrected total	7145	893			

Green and pink shaded areas in Figure 4 indicate the comfort temperature zone and the safety zone at 2 m/s, respectively. In Figure 4, it appears that RH has little impact on the size of the tolerance zone and comfort zone when RH is above 70%.

3.2. Economic Analysis of Localized Cooling under Deep Mine

Using Jiahe Mine’s 9435 working face as an example, as seen in Figure 5, the localized cooling of working faces was evaluated for economic feasibility. Located at a depth of –1000 m, the 9435 working face with a tunnel perimeter of 8.6 m has a rock temperature of 34 °C and an inlet DBT of 37.4 °C. The thermoregulation device is an air–water heat exchanger installed on one side of the tunnel, cooling the working area. According to Figure 6, hot and humid air (point W) partially enters the thermoregulation device and is

refrigerated by cold water circulating in the pipes. The cooled air (point O) mixes with the hot and humid air (point N), with N being the appropriate state for workers.

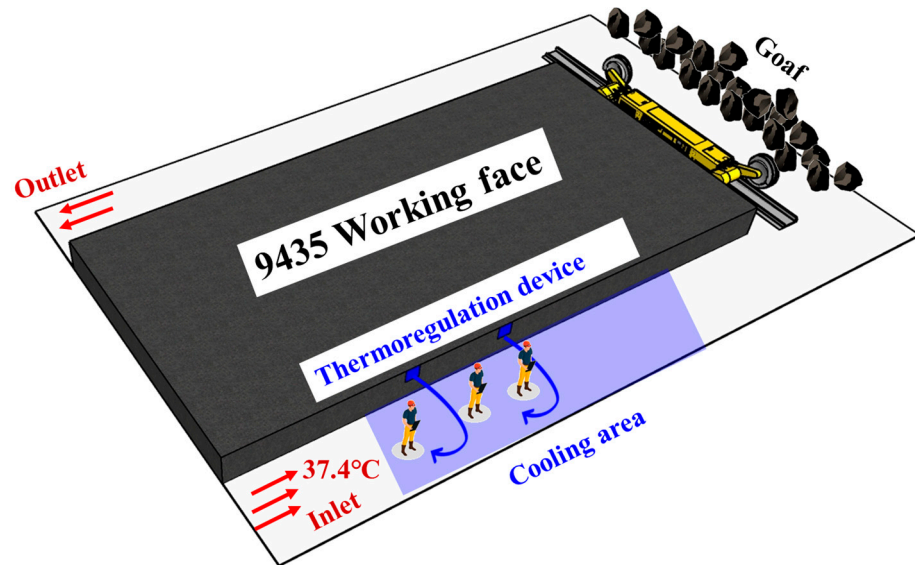


Figure 5. Localized cooling in the 9435 working face.

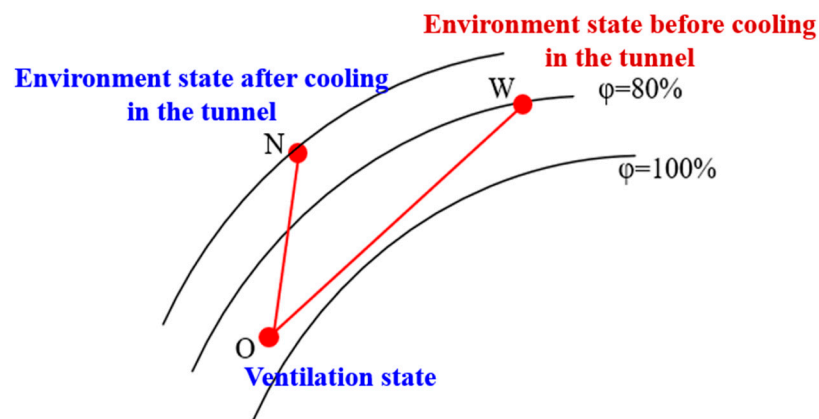


Figure 6. Air handling process of localized cooling.

Six miners worked in a tunnel measuring 300 m in length that required cooling in this area. The operating cost would be predicted by Equations (27) and (28). Calculations of sensible and latent heat are presented in Tables 12 and 13.

Table 12. Sensible heat loads when the DBT is 26–31 °C and RH is 80%.

DBT (°C)	Equipment Load (W)	Staff Load (kW)	Ventilation Load (kW)	Surrounding Rock Heat Dissipation (W)	Total Sensible Heat Load (kW)
26	1200	1.2	253.10	11,022.88	264.57
27	1200	1.2	230.90	9795.02	241.30
28	1200	1.2	208.70	8567.16	217.63
29	1200	1.2	186.49	7339.30	194.20
30	1200	1.2	164.29	6111.44	170.77
31	1200	1.2	142.09	4883.58	147.34

Table 13. Latent heat loads when DBT is 29 °C.

RH (%)	Personnel Loose Moisture (W)	Ventilation Latent Heat Load (kW)	Moisture Loss of Surrounding Rock (kW)	Total Latent Heat Load (kW)
60	0.26	129.61	3.97	136.51
65	0.26	113.73	3.47	119.80
70	0.26	97.76	2.98	103.00
75	0.26	81.70	2.48	86.10
80	0.26	65.54	1.98	69.11
85	0.26	49.29	1.49	52.03
90	0.26	32.94	0.99	34.86
95	0.26	16.50	0.50	17.58

$$E_w = \frac{L_{od}}{COP_R} \tag{28}$$

E_w —Theoretical power consumption of refrigeration unit, kW;

L_{od} —Total sensible heat load of the system, kW;

COP_R —Coefficient of performance of refrigerator, multi-purpose screw refrigerator, take 4.7;

Then, obtain the annual cooling cost per ton of coal according to the electricity fee.

$$F_w = \frac{n \cdot E_w \cdot F_d}{D_t} \tag{29}$$

F_w —Annual cooling cost per ton of coal, RMB/t;

F_d —electricity price, RMB/kW·h;

n —annual operating time, h;

D_t —The annual coal mining volume of the working face, t;

Figures 7 and 8 show that the cooling operation cost and the maximum WBT for the 6- and 8-hour working periods can be calculated. The article suggested that the cost and WBT would have changed little when the air velocity exceeded 2 m/s. Consequently, the recommendation for air velocity would be 2 m/s, with the maximum WBT being 28 °C for six hours and 26 °C for eight hours.

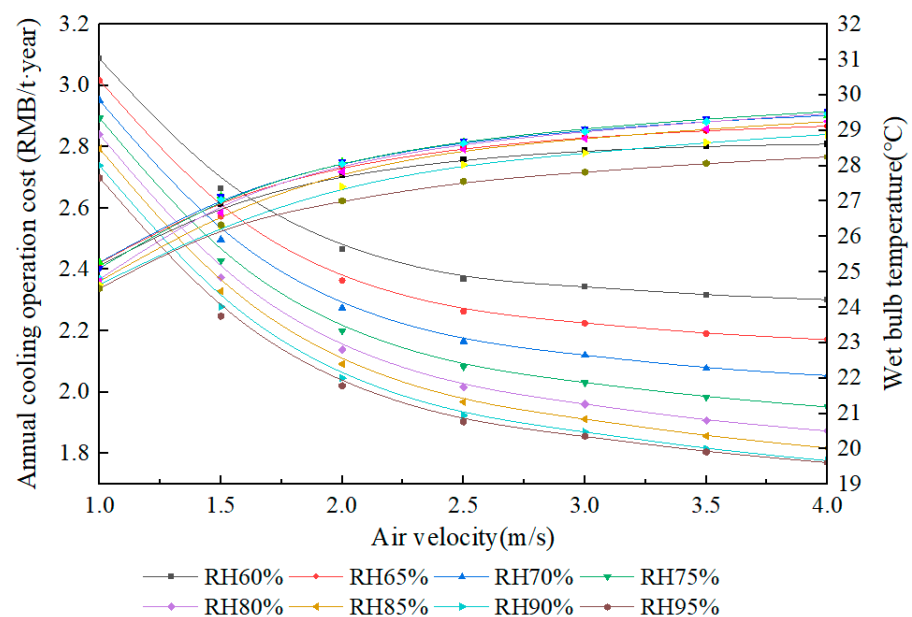


Figure 7. Annual cooling operation cost and WBT with the 6-hour working period.

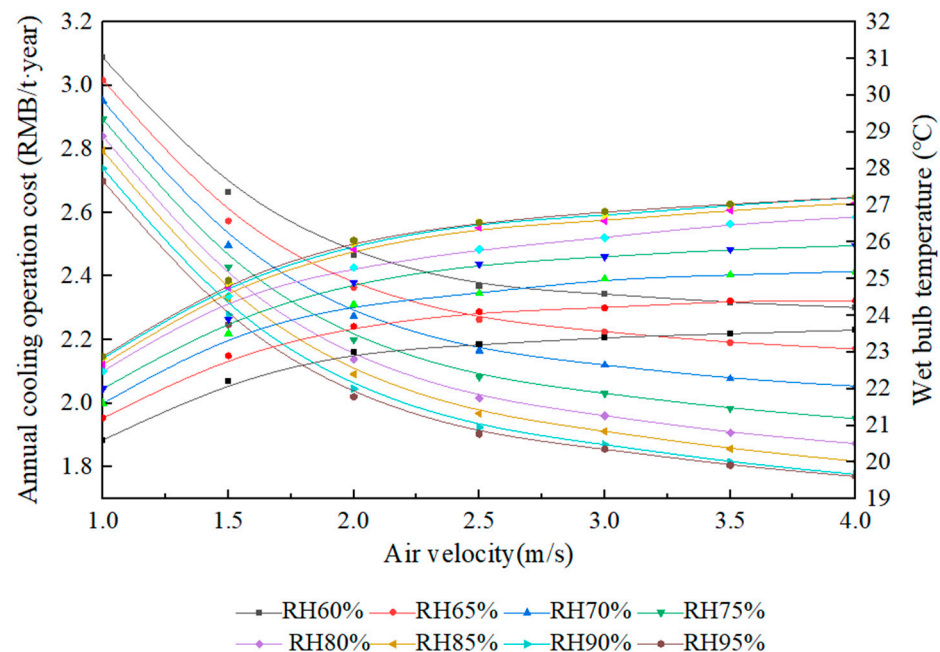


Figure 8. Annual cooling operation cost and WBT with the 8-hour working period.

4. Conclusions

Due to deep mining, mechanical cooling systems have been most frequently used to control thermal environments. However, cooling an entire mining tunnel would be a significant energy-intensive process. A reduction in workers and a decline in physical work intensity indicate that localized cooling will be widespread in the future intelligent mining industry. Therefore, the climatic conditions under localized cooling will be studied to protect mining workers. A modified PHS model for a warm and humid climate was presented in the article, along with reasonable and secure environmental parameters. Furthermore, the results are listed as follows.

- (1) The article modified the PHS model to account for warm and humid conditions based on human factors. The metabolic rate, clothing insulation, and evaporation heat resistance of clothing were modified for warm and humid underground environments. Based on the modified PHS model, the duration of miners' exposure was calculated using MATLAB.
- (2) Air temperature was the primary factor affecting underground miners' safety, followed by relative humidity and air velocity. The improvement of the thermal environment by increasing air velocity is directly related to the thermal humidity index; when the thermal humidity index is lower than 32, increased air velocity will achieve a significant cooling effect.
- (3) The recommended air velocity would be 2 m/s, and the maximum temperature of the wet bulb would be 28 °C for a 6-hour working period and 26 °C for an 8-hour working period, taking into account the security of mining workers and the economic efficiency of the cooling system.

This study may contribute to the cooling of intelligent mining and the formulation of cooling standards in China.

Author Contributions: Conceptualization, Q.H.; Software, D.L.; Validation, K.L.; Data curation, W.Y.; Writing—review & editing, X.Y. All authors have read and agreed to the published version of the manuscript.

Funding: Financial support for this project was provided by the National Natural Science Foundation of China (No. 52074295, 42202321), the Scientific Research Foundation of Hunan Education Department (No. 20B217), the National Natural Science Foundation of Hunan (No. 2021JJ30269), and the State Key Laboratory for GeoMechanics and Deep Underground Engineering (No. SKL-GDUEK202217).

Acknowledgments: We also express our sincere appreciation to Liu Xingxing for her help.

Conflicts of Interest: The authors declare no conflict of interest.

References

- Li, J.G.; Zhan, K. Intelligent mining technology for an underground metal mine based on unmanned equipment. *Engineering* **2018**, *4*, 381–391. [\[CrossRef\]](#)
- Wang, M.; Liu, P.; Shang, S.Y.; Chen, Q.; Zhang, B.; Liu, L. Numerical and experimental studies on the cooling performance of backfill containing phase change materials. *Build. Environ.* **2022**, *218*, 109155. [\[CrossRef\]](#)
- Li, S.B.; Li, S.; Zhang, S.X.; Wang, F. Key technology and application of intelligent perception and intelligent control in fully mechanized mining face. *Coal Sci. Tech.* **2021**, *49*, 28–39.
- Crawford, J.A.; Joubert, H.P.R.; Mathews, M.J.; Kleingeld, M. Optimised dynamic control philosophy for improved performance of mine cooling systems. *Appl. Therm. Eng.* **2019**, *150*, 50–60. [\[CrossRef\]](#)
- Vosloo, J.; Liebenberg, L.; Velleman, D. Case study: Energy savings for a deep-mine water reticulation system. *Appl. Energy* **2012**, *92*, 328–335. [\[CrossRef\]](#)
- Twort, C.T.; Lowndes, I.S.; Pickering, S.J. An application of thermal exermal analysis to the development of mine cooling systems. *Proc. Inst. Mech. Eng. Part C J. Mech. Eng. Sci.* **2002**, *216*, 845–857. [\[CrossRef\]](#)
- Belle, B.; Biffi, M. Cooling pathways for deep Australian longwall coal mines of the future. *Int. J. Min. Sci. Technol.* **2018**, *28*, 865–875. [\[CrossRef\]](#)
- Han, Q.Y.; Zhang, Y.; Li, K.Q.; Zou, S.H. Computational evaluation of cooling system under deep hot and humid coal mine in China: A thermal comfort study. *Tunn. Undergr. Space Technol.* **2019**, *90*, 394–403.
- Roghanchi, P.; Kocsis, K.C.; Sunkpal, M. Sensitivity analysis of the effect of airflow velocity on the thermal comfort in underground mines. *J. Sustain. Min.* **2016**, *15*, 175–180. [\[CrossRef\]](#)
- Wang, H.Q.; Zou, Z.Y.; Chen, S.Q.; Li, Y.Q. Improving thermal comfort of high-temperature environment of heading face through dehumidification. *J. Coal Sci. Eng.* **2010**, *16*, 389–393. [\[CrossRef\]](#)
- Wang, S.G.; Xu, Z.; Zhang, T.F.; Liang, Y.T. Human thermal comfort for mine environment. *J. China Coal Soc.* **2010**, *35*, 97–100.
- Saunders, A.G.; Dugas, J.; Tucker, R.; Lambert, M.; Noakes, T. The effects of different air velocities on heat storage and body temperature in humans cycling in a hot, humid environment. *Acta. Physiol. Scand.* **2005**, *183*, 241–255. [\[CrossRef\]](#) [\[PubMed\]](#)
- Paloma, L.; Moe, M. Development of a modified predicted heat strain model for hot work environments. *Int. J. Min. Sci. Technol.* **2020**, *30*, 477–481.
- Sasmito, A.P.; Kurnia, J.C.; Birgersson, E.; Mujumdar, A.S. Computational evaluation of thermal management strategies in an underground mine. *Appl. Therm. Eng.* **2015**, *90*, 1144–1150. [\[CrossRef\]](#)
- Nie, X.X.; Wang, T.Y.; Sun, F.G.; Wang, Z. Influence of Heat and Humidity Environment on Function of Human Body in High Temperature Mine. *Metal Mine* **2020**, *526*, 186–193.
- Talebi, E.; Sunkpal, M.; Sharizadeh, T.; Roghanchi, P. The Effects of Clothing Insulation and Acclimation on the Thermal Comfort of Underground Mine Workers. *Min. Metal Explor.* **2020**, *37*, 1827–1836. [\[CrossRef\]](#)
- Kalkowsky, B.; Kampmann, B. Physiological strain of miners at hot working places in German coal mines. *Ind. Health* **2006**, *44*, 465–473. [\[CrossRef\]](#)
- Zhang, J.G.; Yang, S.H.; Suo, C.Y. Research on effects of high temperature and high humidity environment on miners physiology and psychology. *J. China Saf. Sci.* **2015**, *25*, 23–28.
- Zhang, C.; Tang, S.C.; Li, D.M.; Xing, J.J.; Xu, A.M.; Li, J. Experimental study of the heavy-duty working condition and intensified fatigue grade for the workmen under high temperature and great humidity environment. *J. Saf. Environ.* **2015**, *15*, 176–180.
- Wu, J.S.; Fu, M.; Tong, X.; Song, H.T.; Kong, S. Evaluation on heat strain of mine worker in high temperature and high humidity mine. *Coal Sci. Tech.* **2015**, *43*, 30–36.
- Du, C.Q.; Li, B.Z.; Li, Y.Q.; Xu, M.N.; Yao, R.M. Modification of the Predicted Heat Strain (PHS) model in predicting human thermal responses for Chinese workers in hot environments. *Build. Environ.* **2019**, *165*, 106349. [\[CrossRef\]](#)
- Sunkpal, M.; Roghanchi, P.; Kocsis, K.C. A Method to Protect Mine Workers in Hot and Humid Environments. *Saf. Health Work* **2017**, *9*, 149–158. [\[CrossRef\]](#) [\[PubMed\]](#)
- Chu, Z.; Zhou, G.; Rao, Z.; Wang, Y.; Zhao, X. Field measurement and assessment on airflow thermodynamic parameters in hot and humid underground tunnelling: A case study. *Tunn. Undergr. Space Technol.* **2022**, *121*, 104341. [\[CrossRef\]](#)
- Li, Z.J.; Xu, Y.; Li, R.R.; Jia, M.T.; Wang, Q.L.; Chen, Y.; Cai, R.Z.; Han, Z.Q. Impact of the water evaporation on the heat and moisture transfer in a high-temperature underground roadway. *Case Stud. Therm. Eng.* **2021**, *28*, 101551. [\[CrossRef\]](#)
- Wang, J.; Du, C.; Wang, Y. Study on the influence of ventilation parameters on the airflow temperature in excavation roadway and ventilation duct. *Case Stud. Therm. Eng.* **2021**, *28*, 101387. [\[CrossRef\]](#)

26. Wei, D.; Du, C.; Lin, Y.; Chang, B.; Wang, Y. Thermal environment assessment of deep mine based on analytic hierarchy process and fuzzy comprehensive evaluation. *Case Stud. Therm. Eng.* **2020**, *19*, 100618. [[CrossRef](#)]
27. Li, J.; Song, F.M.; Cheng, C.X. Study on continuous working time of mine personnel in high temperature and high humidity environment. *Min. Saf. Environ. Prot.* **2021**, *48*, 112–115.
28. Zuo, Q.M.; Cheng, W.M.; Miao, D.J.; Wang, G. Fuzzy Synthetic Evaluation of Thermal Environment of High Temperature Mine Based on Heat Hazard Effects on People. *Saf. Coal Min.* **2009**, *40*, 86–89.
29. Fanger, P.O. *Thermal Comfort-Analysis and Applications in Environmental Engineering*; Danish Technical Press: Copenhagen, Denmark, 1970.
30. Long, S.Z. *Research on Theory and Application of Human-Machine-Environment System Engineering*; Science Press: Beijing, China, 2004.
31. González-Alonso, J. Influence of body temperature on the development of fatigue during prolonged exercise in the heat. *J. Appl. Physiol.* **1999**, *86*, 1032–1039. [[CrossRef](#)]
32. Hao, X.L.; Guo, C.X.; Lin, Y.L.; Wang, H.Q.; Liu, H.Q. Analysis of heat stress and the indoor climate control requirements for movable refuge chambers. *Int. J. Environ. Res. Public Health* **2016**, *13*, 518. [[CrossRef](#)]
33. Werner, J.; Buse, M. Temperature profiles with respect to inhomogeneity and geometry of the human body. *J. Physiol.* **1988**, *65*, 1110–1118. [[CrossRef](#)] [[PubMed](#)]
34. Qu, J.T.; Zeng, F.X.; Feng, W.P.; Li, X. Difference of energy consumption in high temperature and high humidity environment and normal temperature environment. *Chin. J. Sports Med.* **2015**, *34*, 164–169.
35. Tian, S.C.; Zhou, R.K.; Yang, J. Effects of cooling garments on firefighter's thermal responses under high temperature. *China Saf. Sci. J.* **2020**, *30*, 166–171.
36. Sudo, M.; Murakami, S.; Kato, S.; Song, D. Study on the personal air-conditioning system considering human thermal adaptation (Part 7)-thermal comfort and response time to thermal stimulus given from change of activity. *The Society of Heating, Air-Conditioning Sanitary Engineers of Japan*, 2004.
37. Hall, J.R.J.F.; Polte, J.W. Effect of water content and compression on clothing insulation. *J. Appl. Physiol.* **1956**, *8*, 539–545. [[CrossRef](#)] [[PubMed](#)]
38. Yang, X.Q.; Sun, Y.C.; Pei, Y.F. The influence of water containing rate on the thermal comfort of fabric. *Prog. Text. Sci. Technol.* **2008**, *1*, 61–63.
39. Shapiro, Y.; Pandolf, K.B.; Goldman, R.F. Predicting sweat loss response to exercise, environment and clothing. *Eur. J. Appl. Physiol. Occup. Physiol.* **1982**, *48*, 83–96. [[CrossRef](#)] [[PubMed](#)]
40. Wu, Q.Q.; Liu, J.H.; Zhang, L.; Zhang, J.W.; Jiang, L.L. Effect of temperature and clothing thermal resistance on human sweat at low activity levels. *Build. Environ.* **2020**, *183*, 107117.
41. Mehnert, P.; Bröde, P.; Griefahn, B. Gender-related difference in sweat loss and its impact on exposure limits to heat stress. *Int. J. Ind. Ergonom.* **2002**, *29*, 343–351. [[CrossRef](#)]
42. Yang, X.J.; Han, Q.Y.; Pang, J.W.; Shi, X.W.; Hou, D.J.; Liu, C. Progress of heat-hazard treatment in deep mines. *Min. Sci. Technol.* **2011**, *21*, 295–299.
43. Zhu, N.; Chong, D. Evaluation and improvement of human heat tolerance in built environments: A review. *Sustain. Cities Soc.* **2019**, *51*, 101797. [[CrossRef](#)]
44. Zou, S.H.; Li, K.Q.; Han, Q.Y.; Yu, C.W. Numerical simulation of the dynamic formation process of fog-haze and smog in transport tunnels of a hot mine. *Indoor Built Environ.* **2017**, *26*, 1062–1069. [[CrossRef](#)]

Disclaimer/Publisher's Note: The statements, opinions and data contained in all publications are solely those of the individual author(s) and contributor(s) and not of MDPI and/or the editor(s). MDPI and/or the editor(s) disclaim responsibility for any injury to people or property resulting from any ideas, methods, instructions or products referred to in the content.